Developmental Biology 478 (2021) 13–24

Contents lists available at ScienceDirect

Developmental Biology

journal homepage: www.elsevier.com/locate/developmentalbiology

Light-induced, spatiotemporal control of protein in the developing embryo of the sea urchin

Florence D.M. Wavreil [1], Jessica Poon [1], Gary M. Wessel, Mamiko Yajima [*]

Department of Molecular Biology, Cell Biology, and Biochemistry, Brown University, 185 Meeting Street, BOX-GL277, Providence, RI, 02912, USA

ARTICLE INFO

Keywords:
Kaede
CALI
Photoconvertible protein
Embryonic development
Sea urchin embryo

ABSTRACT

Differential protein regulation is a critical biological process that regulates cellular activity and controls cell fate determination. It is especially important during early embryogenesis when post-transcriptional events predominate differential fate specification in many organisms. Light-induced approaches have been a powerful technology to interrogate protein functions with temporal and spatial precision, even at subcellular levels within a cell by controlling laser irradiation on the confocal microscope. However, application and efficacy of these tools need to be tested for each model system or for the cell type of interest because of the complex nature of each system. Here, we introduce two types of light-induced approaches to track and control proteins at a subcellular level in the developing embryo of the sea urchin. We found that the photoconvertible fluorescent protein Kaede is highly efficient to distinguish pre-existing and newly synthesized proteins with no apparent phototoxicity, even when interrogating proteins associated with the mitotic spindle. Further, chromophore-assisted light inactivation (CALI) using miniSOG successfully inactivated target proteins of interest in the vegetal cortex and selectively delayed or inhibited asymmetric cell division. Overall, these light-induced manipulations serve as important molecular tools to identify protein function for for subcellular interrogations in developing embryos.

1. Introduction

Light-induced approaches are powerful tools to track, activate, or extinguish a protein of interest with spatial and temporal control. Many of these technologies were originally developed to manipulate neurons to study protein function and neural networks (Qi et al., 2012; Lin et al., 2013; Sano et al., 2014). In this report, we employ similar approaches in the developing embryo of the sea urchin. Many proteins undergo dynamic expression, localization, and degradation during embryonic development, which is considered to be essential for cell fate specification and differentiation through multiple cell divisions. In the field of developmental biology, however, conventional gene/protein knockdown approaches are often performed in the zygote and its knockdown effect persists in the entire embryo throughout embryogenesis. Therefore, functional contributions of each protein especially at a subcellular level or with a spatial and temporal consideration have often been untested and overlooked because of technical hurdles. Light-induced approaches have great potential to overcome these hurdles by providing methodology to dissect protein dynamics and function at a subcellular level with a temporal control. We previously demonstrated the LOV-ePDZ based optogenetic technique as a promising approach to spatially and temporally control protein localization during embryogenesis of the sea urchin (Uchida and Yajima, 2018). In this technical report, we extend our studies to test additional light-induced approaches, each of which has distinct advantages for specific applications.

One of the approaches we test here uses photoconvertible proteins. Among various photoconvertible proteins available in the field, Kaede and Dendra2 are reported to be photoconverted with only a short-pulse of UV irradiation (McKinney et al., 2009). This photoconversion sensitivity is essential in embryonic cells that are often easily harmed by UV light. Un-photoconverted Kaede and Dendra2 both emit green fluorescence and are irreversibly photoconverted by UV light to fluoresce red (Ando et al., 2002; Mizuno et al., 2003; Adam et al., 2009; McKinney et al., 2009). This makes Kaede and Dendra2 useful tools to monitor the movement of a specific subset of proteins of interest within a cell. This approach can also be used to identify protein turnover and new protein synthesis by measuring both decreasing red fluorescence and increaseing green fluorescent signal overtime after photoconversion (Schmidt et al., 2014; Wolf et al., 2013).

The second approach we test here uses Chromophore-Assisted Light

* Corresponding author.
E-mail address: mamiko_yajima@brown.edu (M. Yajima).
[1] These authors contributed equally.

https://doi.org/10.1016/j.ydbio.2021.06.006
Received 15 March 2021; Received in revised form 10 June 2021; Accepted 12 June 2021
Available online 18 June 2021

Inactivation (CALI). CALI is a microscopic technique that selectively inactivates the function of a protein in a spatiotemporally-controlled manner (Jay, 1988; Diamond et al., 1993; Liao et al., 1994) and has been successful in various cell types (Tour et al., 2003). In this technique, the protein of interest is fused to a photosensitizer (e.g. EGFP, KillerRed, miniSOG) that generates chromophore damage and reactive oxygen species (ROS), thereby causing inactivation and/or destruction of the protein upon laser irradiation of the specific wavelength. Since ROS have a very short lifetime, a focused laser pulse will only affect the molecules in close proximity to the origin of the ROS (~10 nm), allowing for the spatial and temporal inactivation of target proteins (Jacobson et al., 2008; Sano et al., 2014).

To test efficacy of these technologies in the context of subcellular protein regulation during embryonic development, we here use the sea urchin embryo as a model system. This embryo undergoes rapid cell divisions, every 30–40 min, due to a lack of G-phases. In each of the embryonic cells, proteins are differentially expressed and localized subcellularly through each cell division, serving as an ideal model to study spatiotemporal function of proteins essential for embryonic development. Using these sea urchin embryos in this technical report, we demonstrate how light-induced approaches could provide an additional level of analyses for subcellular protein dynamics and function.

2. Materials and methods

2.1. Egg collection and embryo culture

Adult sea urchins, *Strongylocentrotus purpuratus (Sp),* were obtained from Pete Halmay (peterhalmay@gmail.com), Kerchoff Marine Laboratories, California Institute of Technology or from Josh Ross, South Coast Bio-Marine LLC. Long Beach, California, USA. Eggs and sperm were collected by injection of 0.5 M KCl to induce spawning. Sperm were collected dry and eggs were prepared for microinjection by de-jellying them with pH4 seawater (SW). De-jellied eggs were then fertilized in 1 mM 3-aminotriazol (Sigma, St. Louis, MO, USA) to prevent the cross-linking of fertilization envelopes and injected with mRNAs of interest. These injected fertilized eggs were cultured in SW at 16 °C in the dark until they reached the desired stage.

2.2. Construct design and generation

The host constructs were previously made in the pSP64 vector that is optimized for *in vitro* transcription (IVT): GFP (Uchida and Yajima, 2018), Vasa-GFP/mCherry (Yajima and Wessel, 2015), GFP-AGS (modified from AGS-GFP; Poon et al., 2019), Kaede (Poon et al., 2019), GFP-β-catenin. Kaede was amplified by PCR and subcloned into the 5′ end of the gene of interest as represented in Fig. 1B. Similarly, Dendra2 (Addgene #54694) was subcloned as described above to construct pSP64-Deandra2-Vasa. β-Catenin (SPU_009155) open reading frame was PCR-amplified from *Sp* cDNA and subcloned into the pSP64-GFP host vector to construct pSP64-GFP-β-catenin. pCS2-2xmCherry-EMTB was obtained at Addgene (Addgene #26742) (Miller et al., 2009). A miniSOG fragment (318 bp) was PCR-amplified and inserted in frame into each of those host constructs at the 5′ or 3' end of each gene of interest. The original miniSOG fragment was obtained from Addgene (#54821, miniSOG-C1). All subcloning procedures were performed using In-Fusion HD Cloning kit (Takara).

2.3. mRNA preparation and microinjection

Each construct was linearized overnight with *Sal*I, *Sma*I or *Not*I, purified, and subject to IVT using the mMESSAGE mMACHINE® SP6 Transcription Kit (Thermo Fisher; catalog #AM1340) by following the manufacturer's protocol. The injection solution was prepared for a final concentration of 250–1500 ng/μl for each construct. Morpholino antisense oligo for AGS (Poon et al., 2019) was injected with a final concentration of 0.5 mM. Embryos were injected with 6–10 pL of injection mixture and cultured up to the desired stages post fertilization (hpf) at 16 °C.

2.4. Embryo preparation and light activation by confocal microscopy and data analysis

Embryos were cultured in the dark until the 8–16 cell stage (4 hpf) in a glass-bottom dish and then subjected to live imaging. Live confocal imaging was conducted with an Olympus multiphoton microscope for Kaede-photoconversion, Olympus FV3000 point-scanning and Nikon CSU-W1 Spinning Disk laser confocal microscopes for CALI experiments. All of these microscopes are equipped with a software application that allows fine control of light activation, followed by imaging. The embryo was imaged with a Z-stack of 1 μm intervals (2 slices per image for Kaede photoconversion and ~40 slices per image for CALI experiments), processed for higher resolution images, and subject to 2D-projection for quantitative analysis. Quantitative analysis was performed using *Image J*. Statistical analysis was performed by PRISM (GraphPad) using one-way ANOVA followed by Tukey post hoc test. P values less than 0.05 were considered significant. Asterisks were used to indicate significance values where * is $p < 0.05$, ** is $p < 0.01$, *** is $p < 0.001$, **** is $p < 0.0001$. Columns represent means ± SD or SEM.

3. Results and discussion

3.1. Photoconversion dissects pre-existing protein from newly synthesized protein at subcellular level

Kaede and Dendra2 proteins are becoming increasingly useful due to their low cytotoxicity and bright fluorescence for both unphotoconverted (green) and photoconverted (red) proteins. They both fluoresce green when translated, whereas their photoconverted form exhibits red fluorescence (Ando et al., 2002). Kaede exists *in vivo* as a homotetramer, which may affect the morphology and function of a labeled structure (Campbell et al., 2002). On the other hand, Dendra2 is reported to exist as a monomer or as a dimer at high concentration (Adam et al., 2009; Fron et al., 2013). It is, however, reported to have slower photoconversion rates in some model systems compared to Kaede, which may increase a risk of photobleaching or cytotoxicity (Shaner et al., 2007; Rausin et al., 2010; Wei et al., 2011; Jasik et al., 2013). Therefore, each photoconvertible protein has *pros* and *cons* which need to be evaluated for each application.

In this report, we selected Kaede and Dendra2 for photoconversion due to their bright fluorescence and reported sensitivity for photoconversion considering embryos are highly sensitive to light irradiation. To test their efficacy, we first performed photoconversion under the epifluorescence widefield microscope. UV-exposure changed the color within a second for Kaede and within a few seconds for Dendra2 (data not shown), highlighting their sensitivity. To have better control of UV irradiation, laser microscopy was employed for the rest of the experiments even though both proteins are easily photoconverted and appear not to cause any toxicity due to the minimum light irradiation needed (data not shown).

To test if Kaede and Dendra2 could successfully mimic the endogenous protein expression pattern, each of the proteins was fused to Vasa, an RNA helicase. This protein was selected as a test molecule because it shows dynamic yet specific subcellular localization on the spindle during M-phase and becomes enriched into the micromere lineage through an asymmetric cell division at the 16-cell stage (Yajima and Wessel, 2011b) (Fig. 1A). The Vasa open reading frame (ORF) was fused to Kaede or Dendra2 to construct a fusion protein (Fig. 1B), and the cognate mRNA was microinjected into fertilized eggs of the sea urchin *S. purpuratus.* At the 16-cell stage, both the Kaede- and Dendra2-Vasa successfully mimicked endogenous Vasa or Vasa-GFP protein expression patterns on the spindle as well as asymmetric enrichment at the vegetal cortex

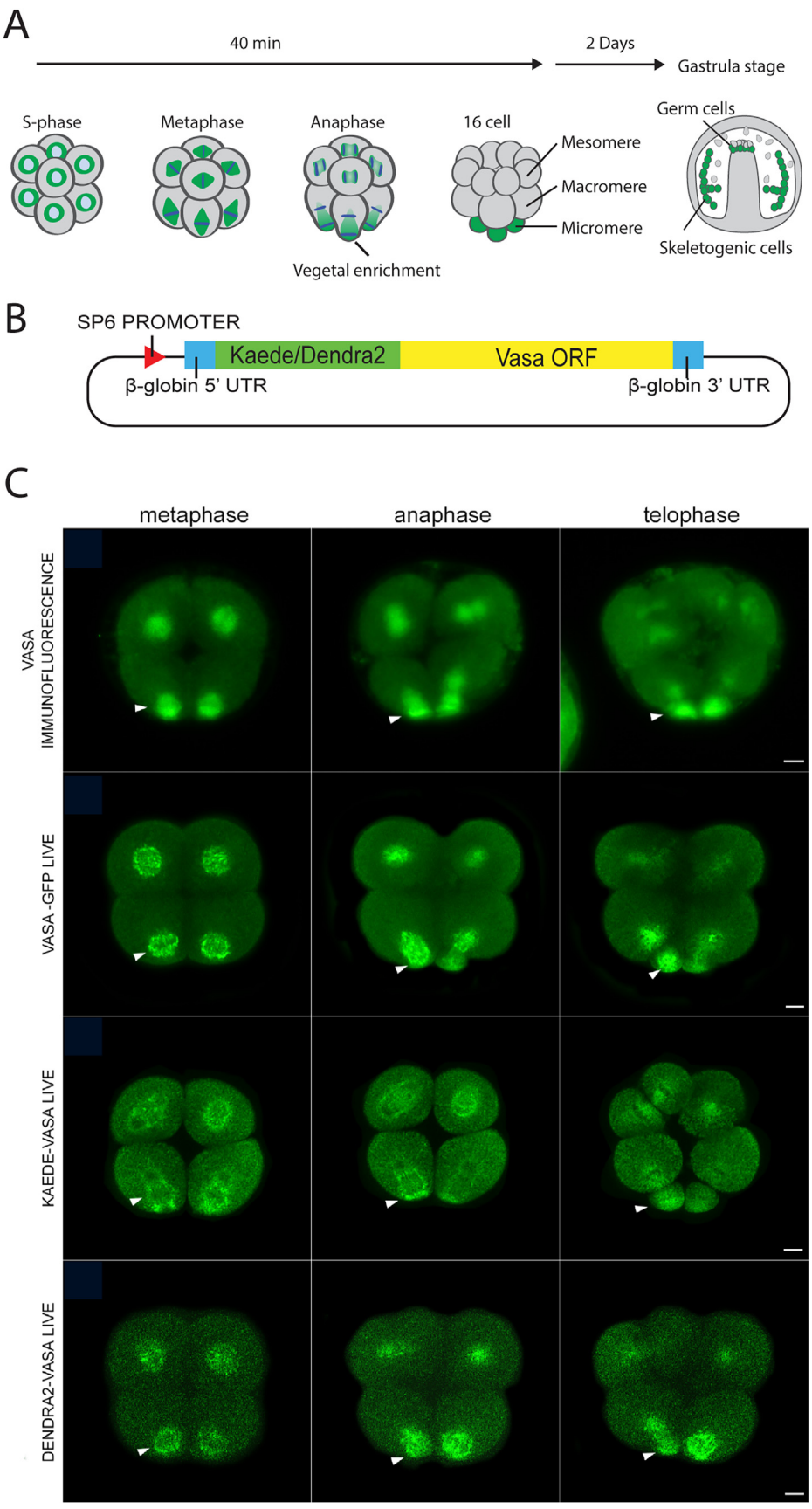

Fig. 1. (A) A schema depicting Vasa (green) localization during early embryogenesis. (B) Construct design of Kaede/Dendra2-Vasa plasmid. (C) The Kaede/Dendra2-Vasa successfully mimicked endogenous Vasa (Vasa immunofluorescence) or Vasa-GFP expression patterns as previously reported. Arrowheads indicate Vasa protein enrichment. Vasa protein level is titrated by the protein degradation mechanisms, and thus Vasa mRNA overexpression causes no developmental defect, making this construct a useful tool to track the protein dynamics. Scale bar = 20 μm. The number of embryos observed for each sample group is: Kaede-Vasa n = 105, Dendra2-Vasa n = 55, Vasa-GFP n = 50 and Vasa immunofluorescence n = 121. Scale bars = 20 μm.

(Fig. 1C, arrowheads) as previously reported (Yajima and Wessel, 2011b). However, Kaede-Vasa showed slightly clearer and broader localization patterns, which may be due to the tetrameric nature of this protein. Dendra2-Vasa mimicked the localization pattern more precisely yet its signal generally appeared to be less intense compared to Kaede-Vasa. Both fusion proteins showed no apparent cytotoxicity under normal condition.

To track Vasa dynamics at a subcellular level, we next photoconverted a portion of Kaede-Vasa on the spindle of the animal tier of blastomeres that were undergoing symmetric cell divisions at 8–16 cell stage followed by imaging of a sub Z-section of the embryo (Fig. 2; Supplementary Video 1). Laser irradiation targeted the center region of the selected spindle in the embryo with 405 nm laser (0.5% power) for 250 ms, which immediately resulted in intense red fluorescence of Kaede-Vasa (Fig. 2A). This short exposure minimized any cellular toxicity, and cells exposed to the UV developed normally without any delay in cell cycling compared to non-irradiated sibling cells within a single embryo (compare Fig. 2B, irradiated and C, non-irradiated). The strength of the photoconverted signal diminished over time but stayed restricted to the spindle instead of dispersing into the cytoplasm. Both the photoconverted (red) and the un-photoconverted (green) Kaede-Vasa remained associated with the spindle throughout metaphase and anaphase and were equally distributed on both sides of the spindle (Fig. 2B and C). Quantitative analysis was performed on each side of the spindle in photoconverted and un-photoconverted blastomeres (Fig. 2D). Photoconverted Kaede-Vasa signal on both sides of the spindle showed a decrease at the same rate during this symmetric cell division (Fig. 2D–F). Un-photoconverted levels of Kaede-Vasa on both sides of the spindle were also very similar throughout metaphase and anaphase (Fig. 2G). Since only a sub-section of the z-stack is captured in these experiments, complete 3D-imaging is needed in the future to fully reconstruct this dynamics. However, under this condition, we did not find a marked difference in behaviors of pre-

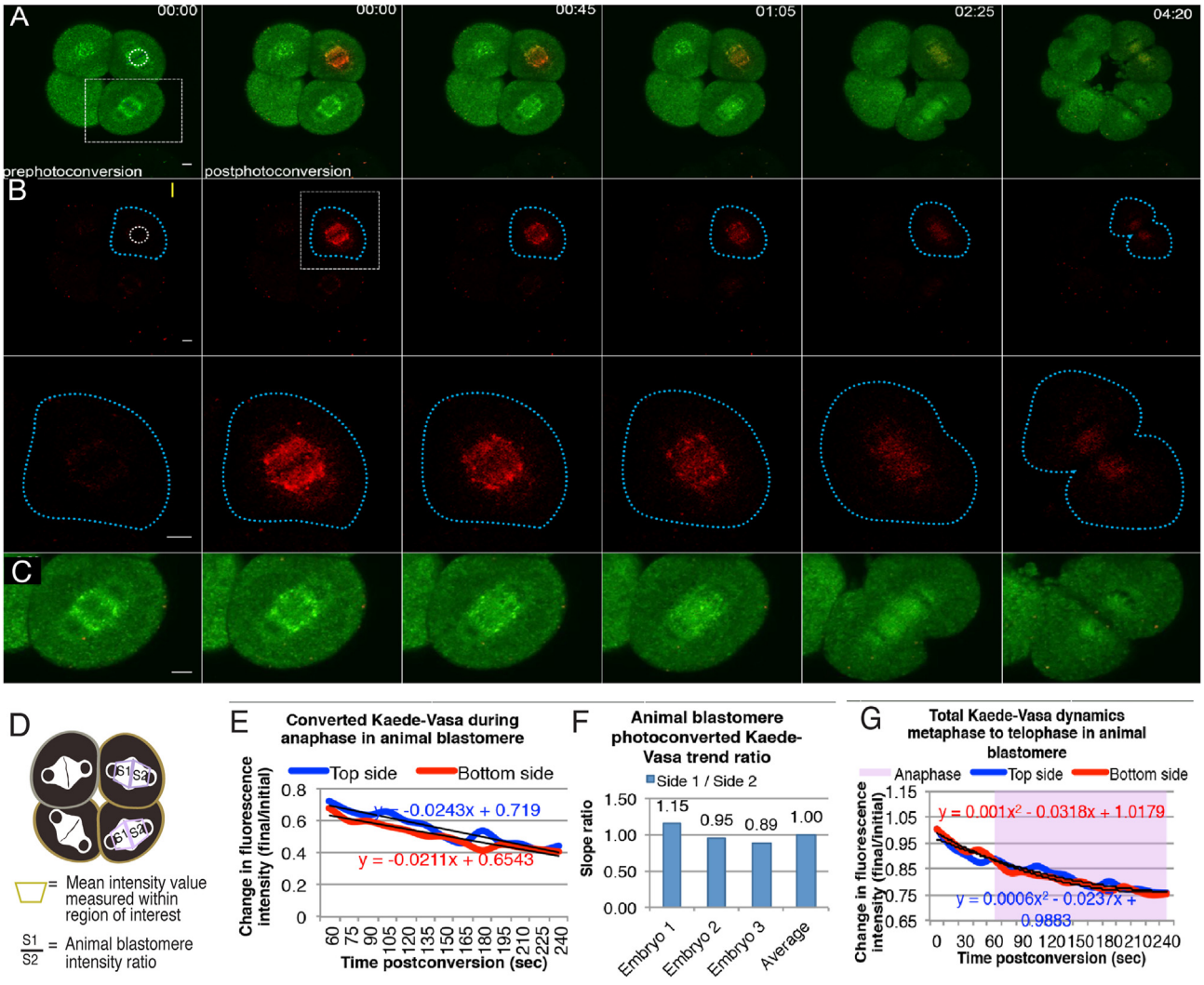

Fig. 2. Photoconverted and un-photoconverted Kaede-Vasa dynamics during symmetric cell division at 8–16 cell stage. (A) Leftmost column shows Kaede-Vasa expression prior to photoconversion (green), while the remaining columns are images taken at varying minute intervals as indicated in the top right corner, following photoconversion (red) during symmetric cell division. (B) Photoconverted Kaede-Vasa fluorescence intensity was high immediately following photoconversion then diminished over time. Photoconverted area was restricted to the spindle rather than the asters (a dashed-line circle). Magnified version (lower panels) shows that the red Kaede-Vasa remained associated with the chromosomes throughout metaphase and anaphase. (C) Magnified (a square region in A), un-photoconverted animal blastomere spindle shows normal Vasa distribution over the course of the cell cycle. (D) A diagram showing the areas and calculation of quantitative analyses. The mean intensity value of Green and Red channels in each region of interest (S1, S2) at each time point was normalized to the value at the start time (Time 0). Intensity ratio on each side of the spindle was calculated by dividing the value of S1 by that of S2. (E) Photoconverted Kaede-Vasa signal on both sides of the spindle in the animal blastomere decreased at the same rate during anaphase. (F) Total levels of Kaede-Vasa on both sides of the spindle in the animal blastomere were very similar throughout metaphase and anaphase. The level on either side did not increase above the initial value. Experiments were repeated at least three times and a representative value out of three individual embryos is shown in each graph. Scale bars = 10 μm.

existing (photoconverted, red) and newly synthesized (un-photoconverted, green) Kaede-Vasa.

A similar trend of Kaede-Vasa behavior was also seen on the spindle during the asymmetric cell division at the vegetal pole during the 8–16 cell stage (Fig. 3A–F; Supplementary Video 2). However, a major difference was seen in the un-photoconverted (green) Kaede-Vasa signal level where the green signal intensity increased overtime at the vegetal cortex during asymmetric cell division (Fig. 3G). Although complete 3D-imaging is again needed to have any mechanistic insight, a difference appears to be present between pre-existing (photoconverted, red) and newly synthesized (un-photoconverted, green) Kaede-Vasa with an increased signal of un-photoconverted signal at the vegetal cortex toward the end of the M-phase. We also performed the same experiment using Dendra2-Vasa and saw the same trend of signal dynamics both for photoconverted and un-photoconverted Dendra2-Vasa during an asymmetric cell division (Fig. 3H–K). However, the photoconverted signal level was much dimmer compared to Kaede-Vasa, making it difficult to image with the low power laser or short exposure time. Although Dendra2-Vasa also showed no apparent cytotoxicity under the same condition, we chose Kaede for the remaining experiments due to its higher signal intensity and readiness of photoconversion. Although it is still not clear how spindle localization of Vasa is regulated in this embryo, these observations suggest at least two possibilities: pre-existing (photoconverted) Vasa may stay on the spindle but gradually degrades or diffuses into the cytoplasm at the same rate toward the end of the M-phase during both symmetric and asymmetric cell divisions. On the other hand, newly synthesized (un-photoconverted) Vasa may increase its protein synthesis or translocate from elsewhere in the vegetal cortex during asymmetric cell division.

Lastly, we also performed and analyzed the same photoconversion experiments using two other proteins of the interest. One is Kaede that shows no specific subcellular localization, which immediately diffused throughout the entire cytoplasm upon photoconversion as expected, resulting in an average intensity level of photoconverted Kaede at each subcellular region measured (Fig. 4A–D; Supplementary Video 3). An additional analysis was performed with Kaede-EMTB (von Dassow et al., 2009) that contains a microtubule-binding domain and thus localizes directly on the microtubules (Fig. 4F–I; Supplementary Video 4). For this experiment, only one side of the spindle was photoconverted. The photoconverted Kaede-EMTB signal remained constant during the entire M-phase, suggesting no active translocation of Kaede-EMTB protein within a spindle. Overall, these observations suggest that each protein indeed appears to undergo different subcellular dynamics in the developing embryonic cells. Although further detailed analyses with complete 3D-scanning of the embryo are needed to quantitatively analyze protein dynamics, these results demonstrate an initial feasibility of Kaede photoconversion to track subcellular protein dynamics in the developing sea urchin embryo.

3.2. CALI specifically depletes CALI-tagged GFP expression

MiniSOG is a photosensitizer that has been used for CALI activation. It is a small (106 amino acids) monomeric protein derived from phototropin 2 of *Arabidopsis thaliana* (Shu et al., 2011). It is most effectively activated at 448 nm although it can also be activated with a common 480 nm GFP filter. Upon blue light irradiation, a singlet oxygen is generated by the flavin mononucleotide embedded within miniSOG, requiring no exogenous cofactor or special laser to induce CALI. MiniSOG is also reported to be more efficient in CALI activation than e.g. EGFP, and does not require a high-power laser, compared to other genetically encoded chromophores such as EGFP (Lin et al., 2013; Sano et al., 2014) and KillerRed (Bulina et al., 2006). For example, fusion of miniSOG to a mitochondrial transporter enabled photoablation of genetically targeted neurons in *Caenorhabditis elegans* without harming other parts of the body due to its high efficiency of singlet oxygen photogeneration (Qi et al., 2012). MiniSOG fusion to VAMP2 – the SNARE complex protein - disrupted presynaptic vesicle release upon blue light irradiation in both cultured neurons and hippocampal organotypic slices (Lin et al., 2013). Further, expression of this miniSOG–VAMP2 fusion protein in whole *C. elegans* neurons causes reduced movement and paralysis upon CALI. This technique has been established to inhibit synapses with CALI (InSynC) (Lin et al., 2013). Therefore, miniSOG has been shown to be an effective CALI factor yet its use has been limited.

Efficacy of CALI has been conventionally assessed by the level of photobleaching, which reflects the level of protein damage caused by laser irradiation (Bulina et al., 2006). To test the efficacy of CALI in the sea urchin embryo, GFP was tagged with miniSOG to construct miniSOG-GFP. Although GFP itself is also known to be sensitive to CALI (Rajfur et al., 2002), we expect to see an increased CALI efficacy in the miniSOG-GFP group compared to the GFP alone. GFP without miniSOG was thus used as a control group. MiniSOG-GFP and GFP mRNAs were introduced into fertilized eggs along with 2xmCherry-EMTB mRNA (Fig. 5A). EMTB binds to microtubules and was used here to counterstain the embryo (von Dassow et al., 2009; Uchida and Yajima, 2018), and mCherry that is insensitive to blue light or CALI was used here as another internal control (Trewin et al., 2018). All experimental procedures were performed for both experimental and control groups at the same time to minimize both technical and batch variances. The injected embryos were then cultured up to the 16-cell stage (4–5 hpf) in the dark and placed on the Olympus FV3000 confocal laser microscope for CALI and imaging. The 488 nm blue laser was applied for 2 s to an entire embryo at a laser power of 0, 15 or 30% followed by imaging at a power of 1–2% for blue and red channels. This protocol was repeated every 10-min for 1–2 cell cycles (~90 min) (Fig. 5B). Imaged embryos were then measured and tracked for the level of the GFP signal in each region of interest (ROI) as well as for the occurrence of cell division at every 5 min. The results showed that the laser irradiation followed by imaging bleached the miniSOG-GFP signal slightly even at 0% power of the CALI laser, yet more significantly at 15 and 30% laser power, while the control GFP instead showed a signal increase even at 30% laser under this condition (Fig. 5C and D). On the other hand, the mCherry-EMTB signal was unaffected in both groups, suggesting a specific decrease of miniSOG-tagged GFP protein. Embryos injected with miniSOG-GFP showed slight cell toxicity detected by spindle disorganization, yet no significant cell cycle delay was observed within this time frame of recording. We also tested CALI with lower laser powers such as 3% and 6%, but the signal decrease in this case was minimal (data not shown).

To test this CALI-dependent bleaching further, we used β-catenin as a test molecule. β-Catenin is a member of the Wnt signaling pathway components and is critical for establishing animal-vegetal (A-V) axis in the sea urchin embryo as well as in many other organisms (Logan and McClay, 1999). Under normal conditions, nuclear β-catenin is enriched in the vegetal cell nuclei from the 32-cell stage (Fig. 6A, control, arrow) and forms a decreasing gradient toward the animal pole. Using the same light activation condition as in Fig. 5A, we found that CALI effectively bleached the GFP signal of miniSOG-tagged GFP-β-catenin compared to the control group (Fig. 6A; Supplementary Video 5). The most effective laser condition in this case was, however, 45% laser power, which may be due to the target molecule being located in the nucleus and far from the cell surface (Fig. 6B; Supplementary Video 6). Under this laser condition with endogenous β-catenin being present in the cell, embryos underwent cell divisions with no apparent delay in cell cycling in both groups. However, the gradient of nuclear β-catenin expression was diminished only in the experimental group, suggesting specific bleaching of β-catenin expression in the developing embryo. These results suggest that the miniSOG-tagged protein is more sensitive to photobleaching and potentially susceptible to light-dependent inactivation compared to the control, which needs to be further tested in the absence of the endogenous protein. These results demonstrate an initial feasibility of this technology in the developing sea urchin embryo.

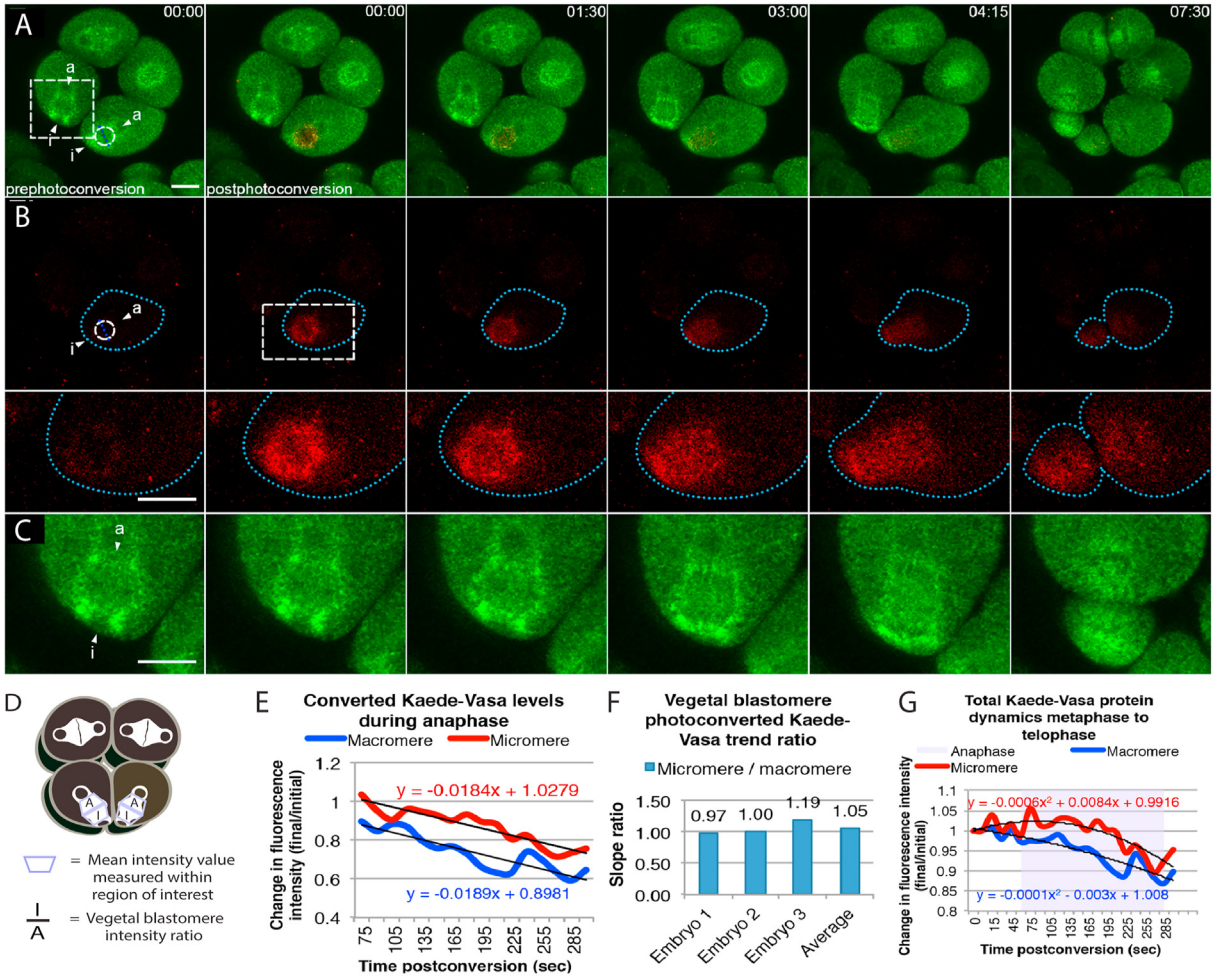

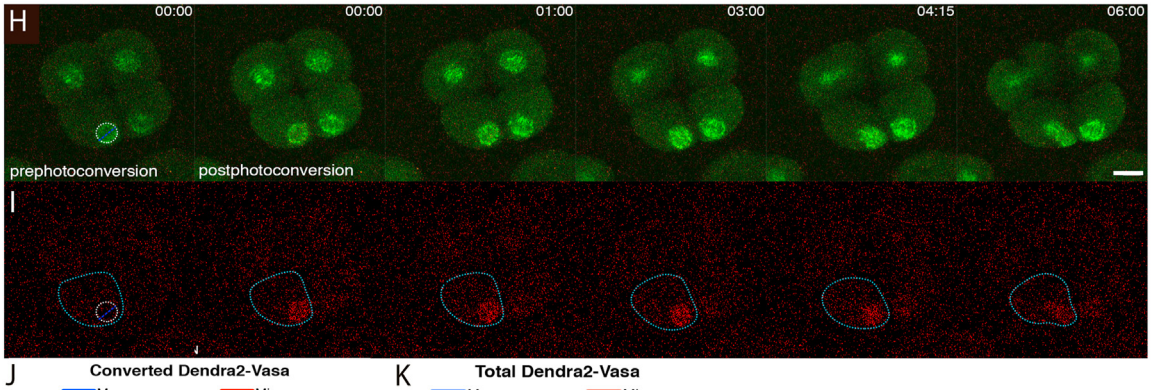

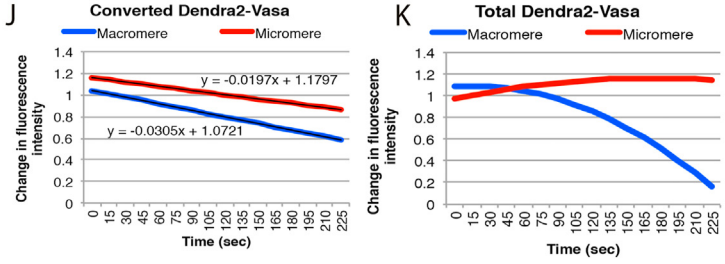

(caption on next page)

Fig. 3. Kaede-Vasa and Dendra2-Vasa dynamics during asymmetric cell division at 8–16 cell stage. (A) Leftmost column shows Kaede-Vasa expression prior to photoconversion (green), while remaining columns are images taken at varying minute intervals as indicated in the top right corner, following photoconversion (red) during asymmetric cell division. The photoconversion was performed in the white-circled region at 8-cell stage metaphase. (B) The red channel and its magnified images of the region circled in the top panels. Photoconverted Kaede-Vasa (red) levels were similar on both the macromere (a) and micromere (i) side of the spindle-complex at metaphase and decreased on both sides of the spindle following photoconversion. A square in the image indicates the vegetal blastomere undergoing micromere formation. (C) The magnified images of the un-photoconverted region squared in A. (F) Photoconverted Kaede-Vasa signal on both the micromere and macromere sides of the spindle during the 8–16 cell stage decreased at similar rates over anaphase. (F) Slope ratios of converted Kaede-Vasa in the micromere and macromere were approximately 1 from 3 different embryos. (G) Total Kaede-Vasa levels on the micromere side of the spindle remained above the initial total Kaede-Vasa level until approximately 2 min after the start of anaphase, and then decreased below after that point. (H–K) Dendra2-Vasa distribution during micromere formation. Un-photoconverted (green) (H) and Photoconverted (red) (I) Dendra2-Vasa localized to the mitotic spindle. The dashed-circle region was photoconverted. (J, K) Photoconverted (J) Dendra2-Vasa decreased on both sides of the spindle, while Total (K) Dendra2-Vasa remained consistent on the micromere side of the spindle during anaphase. n = 3. Experiments were repeated at least three times and a representative value out of three individual embryos is shown in each graph. Scale bars = 15 μm.

3.3. CALI on AGS disturbs asymmetric cell division in the embryo

To test if CALI-dependent photobleaching impacts activity of other proteins of interest, the AGS protein was used as a test molecule. AGS is a polarity factor that localizes to the spindle and is enriched in the vegetal-most cortex during asymmetric cell divisions, playing an essential role in micromere formation (Poon et al., 2019). AGS appears to anchor the micromere-side of the spindle, and its knockdown by morpholino anti-sense oligo (MO) results in the release of spindle anchoring at the vegetal cortex and inhibits micromere formation (Poon et al., 2019). Here we test if AGS inactivation by CALI will mimic this knockdown phenotype (Fig. 7A). This part of the experiment was performed on the Nikon W1 spinning disk laser confocal microscope.

Since endogenous AGS protein may be insensitive to CALI, AGS-MO that was previously demonstrated to specifically knockdown endogenous AGS protein synthesis and function was used to reduce endogenous AGS protein levels (Poon et al., 2019). AGS-MO was also used here because maternally stored AGS mRNA will not be altered by genome-editing technology such as CRISPR/Cas9, thus the AGS-MO is the most effective way to knockdown endogenous AGS protein activity in these early stage sea urchin embryos (Lin and Su, 2015; Shevidi et al., 2017). GFP-miniSOG-AGS mRNA was microinjected with AGS-MO and 2xmCherry-EMTB to view the stage of the cell cycle. As a control group, embryos microinjected only with 2xmChEMTB were prepared. CALI activation was performed right after nuclear envelope breakdown at the 8-to-16 cell transition with a 473 nm laser at a power of 80% for 25 msec per cycle at 100-sec intervals for 16 cycles in total (Fig. 7B). Irradiation was specifically aimed at the vegetal cortex of one vegetal blastomere during micromere formation at 8 to 16-cell stage to see if this laser irradiation releases the vegetal spindle pole from the vegetal cortex and affects micromere formation (Fig. 7C–E, white arc).

In the experimental group, the laser irradiation specifically bleached the cortical AGS signal in the targeted micromeres (Fig. 7D and E, arrow). Under this condition, in the control group (n = 4), the irradiated blastomere always formed micromeres with the same timing as the non-irradiated sibling blastomeres (Fig. 7C; Supplementary Video 7). In the experimental group, on the other hand, four out of thirteen embryos showed delayed micromere formation compared to the non-irradiated sibling blastomere (Fig. 7D; Supplementary Video 8), and four out of thirteen embryos failed to form micromeres while the sibling blastomeres successfully formed micromeres (Fig. 7E; Supplementary Video 9). Collectively, two thirds of the embryos showed compromised asymmetric cell division in the experimental group (Fig. 7F). Of note, embryos with abnormal development, where even the non-irradiated sibling blastomere did not divide properly, were removed from the analysis both from the control and experimental groups.

We also attempted various conditions of CALI to explore its efficacy under different conditions. First, when CALI was performed in embryos that had already entered anaphase, the resultant embryos underwent asymmetric cell division properly (n = 2; data not shown). Second, when the irradiation was less frequent with about 5 min intervals, only two out of six embryos showed delayed micromere formation (n = 6; data not shown). Therefore, the timing and frequency of irradiation appear to be critical for successful inhibition of micromere formation. Lastly, we briefly compared the CALI efficacy of GFP-AGS and GFP-miniSOG-AGS in the context of cortical signal inactivation. In this experiment, the entire imaging frame was selected as ROI, and embryos were irradiated with 473 nm blue light only once at varying laser powers at the 16–32 cell stage. The GFP fluorescence intensity was then measured at the vegetal cortex and the ratio of intensity after and before irradiation was calculated (Supplementary Fig. 1A-B1). Both groups showed a consistent laser power-dependent signal depletion, yet only the 50% laser power showed a significant signal decrease in the GFP-miniSOG-AGS group compared to the GFP-AGS group. At higher laser power, GFP fluorescence was reduced to almost zero for both groups, rendering any statistical significance null. This result is consistent with the earlier results showing that repeated irradiation appears to be rather critical to see a greater CALI effect for both groups over time (Figs. 5 and 6). This may be reasonable considering that embryos are highly three-dimensional and a single irradiation at a single z-plane could be quickly rescued by the neighboring protein in the non-irradiated planes.

Overall, these results suggest that CALI may be an effective approach to directly disrupt asymmetric cell division in developing embryos. Further, cortical AGS appears to be indeed directly responsible for inducing unequal cell division during micromere formation. In previous work, AGS function was tested by its knockdown or overexpression in the entire embryo (Poon et al., 2019), thus its direct role in micromere formation was somewhat unclear. The CALI approach may, therefore, provide a unique advantage to reveal a direct role of a protein of interest by specifically blocking its function in a temporally and spatially targeted manner.

Light-induced approach to control protein activity at a subcellular level with spatial and temporal precision.

The use of light-sensitive proteins such as photoconvertible proteins in the context of embryonic development has been often limited to lineage tracing experiments especially in less-conventional model organisms including echinoderms. In this study, however, we tested the versatility of two light-induced technologies that can be used for quantifying protein dynamics at a subcellular level or for controlling a subcellular event such as asymmetric cell division without causing notable cytotoxicity during embryogenesis of the sea urchin.

To track and quantify subcellular protein dynamics, in this study, we demonstrate Kaede photoconversion as a promising approach. Kaede appears to be sufficiently sensitive for dissecting protein dynamics on time without causing any apparent cytotoxicity or disturbing other subcellular components such as the mitotic spindle. This is particularly critical for embryos with a rapid cell cycle such as the sea urchin embryo that enters M-phase every 20 min in the case of *S. purpuratus*. Due to its sensitivity and speed of conversion (within 250 ms, with 0.5% laser power in this study), Kaede can also be used in a variety of applications such as analyzing protein degradation, translocation, synthesis and interactions of interest at subcellular levels in a combination of complete 3D-imaging. Other photoconvertible proteins such as Photoactivatable (PA)-GFP and PA-mCherry (Subach et al., 2009) were also previously

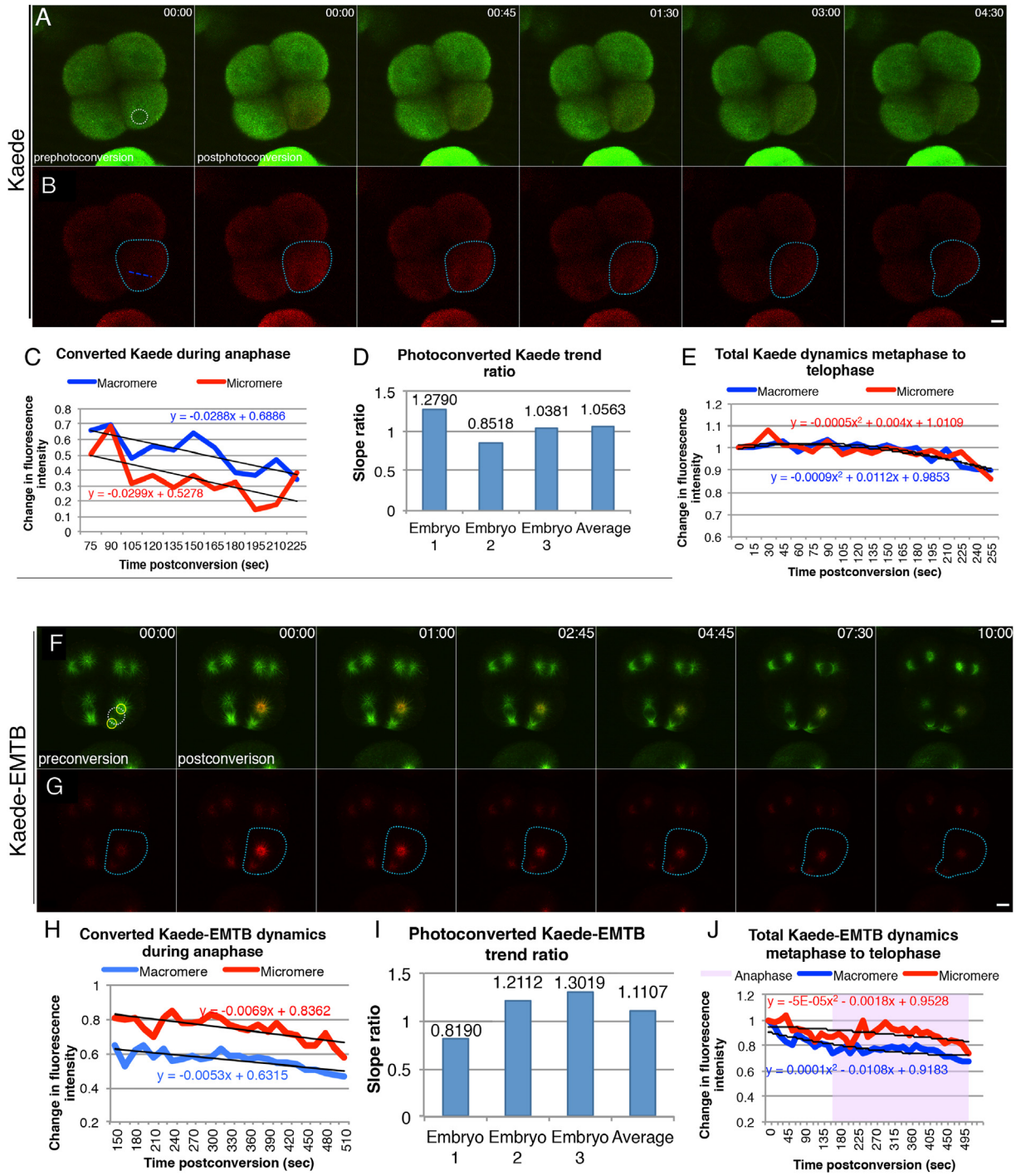

Fig. 4. Distribution of Kaede (A–E) and Kaede-EMTB (F–J) during the 8–16 cell stage. (A–E) Both un-photoconverted (green) (A) and photoconverted (red) (B) Kaede were diffuse throughout each blastomere. On both sides of the vegetal spindle, the red intensities showed a similar decreasing trend (C, D) and the total Kaede intensity stayed constant (E). (F–J) Kaede-EMTB on the macromere side of the spindle (F) and its associated asters were photoconverted (G). (H–J) Photoconverted (H) Kaede-EMTB levels (J) decreased at similar rates on both sides of the spindle during anaphase (I). Total Kaede-EMTB (right graph) on the micromere side of the spindle, however, showed a slightly increasing trend (J). Yellow circles are the regions used for quantitative calculations. Experiments were repeated at least three times and a representative value out of three individual embryos is shown in each graph. Scale bars = 10 μm.

tested in our group. These photoactivatable proteins, however, require a significantly longer UV exposure time (~a few minutes for PA-GFP/mCherry; data not shown) and produce less robust signal. Since protein dynamics in these embryos constantly change, with a timeframe of seconds to minutes, speed and sensitivity to photoconversion is critical for accurate quantification of protein dynamics in real-time. For this specific purpose, Kaede may be one of the optimal tools. Kaede as well as another photoconvertible protein KikGr have been also used in several studies for other purposes such as cell labeling and lineage tracing (Tsutsui et al., 2005; Nowotschin and Hadjantonakis, 2009; Wei et al., 2011; Poon et al., 2019). In these experiments, however, fluorescence of both Kaede and KikGR proteins tends to disappear within a few days due to their natural protein turnover. A fast turnover of the protein could be advantageous for tracking and quantifying protein dynamics in real-time,

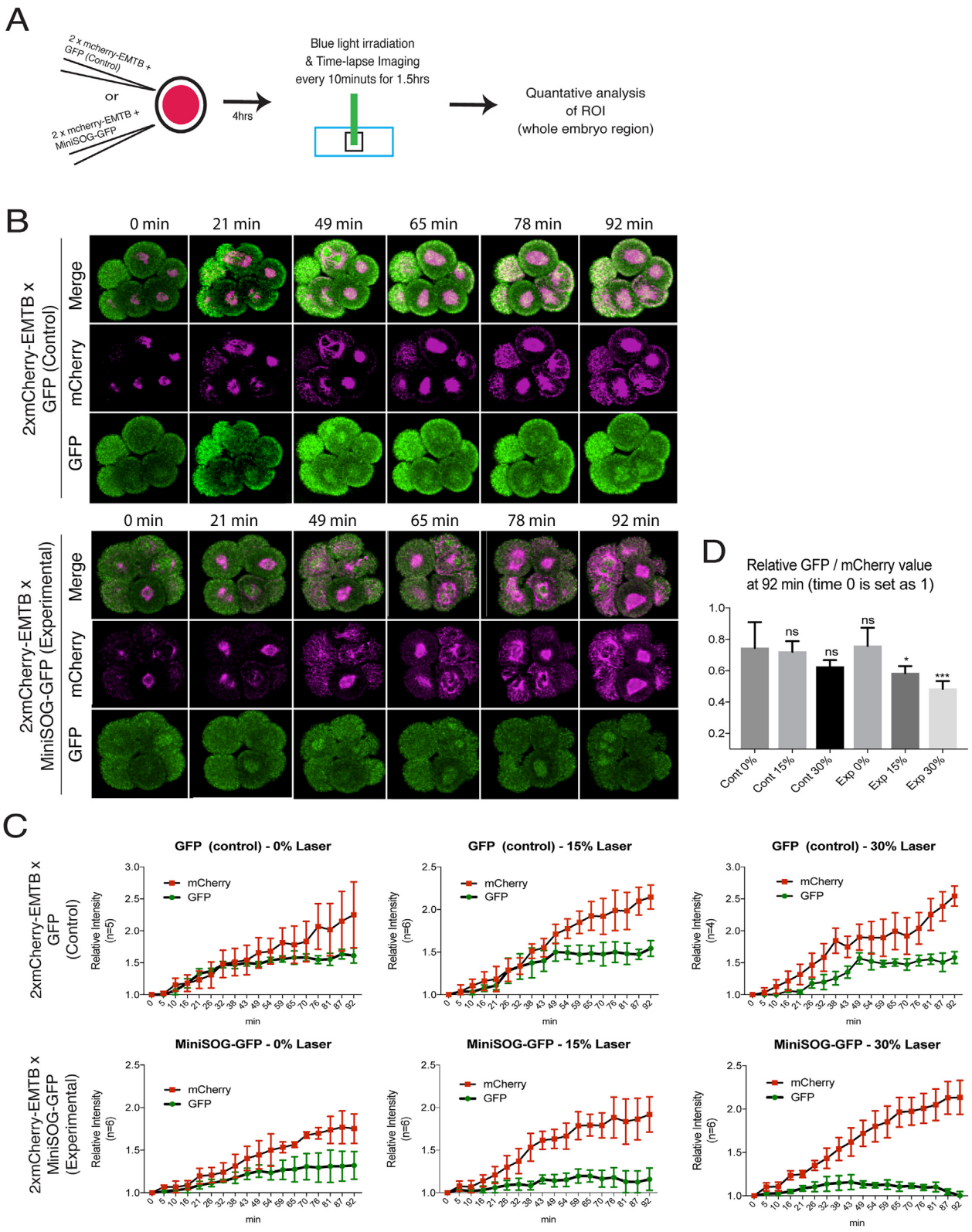

Fig. 5. A blue laser bleaches the miniSOG-GFP signal in a laser power dependent manner. (A) A schematic diagram of the experimental procedure. (B) A time-lapse series of the control (GFP, top panels) and experimental (miniSOG-GFP, bottom) group embryos. Minutes after blue laser irradiation (30%) are indicated at the top of each panel. 2xmCherry-EMTB (microtubule marker, magenta) that is insensitive to CALI was used as a base control. Only the experimental group lost the green signal overtime (C). Average relative intensity of each channel (GFP and mCherry) at each time point was calculated and normalized by that of the corresponding time 0. The embryo group and laser power are indicated at the top of each graph. n indicates the number of embryos analyzed. (D) Average relative intensity value of each embryo group at the time point of 92 min is summarized. n = 4–6. Scale bars = 20 μm.

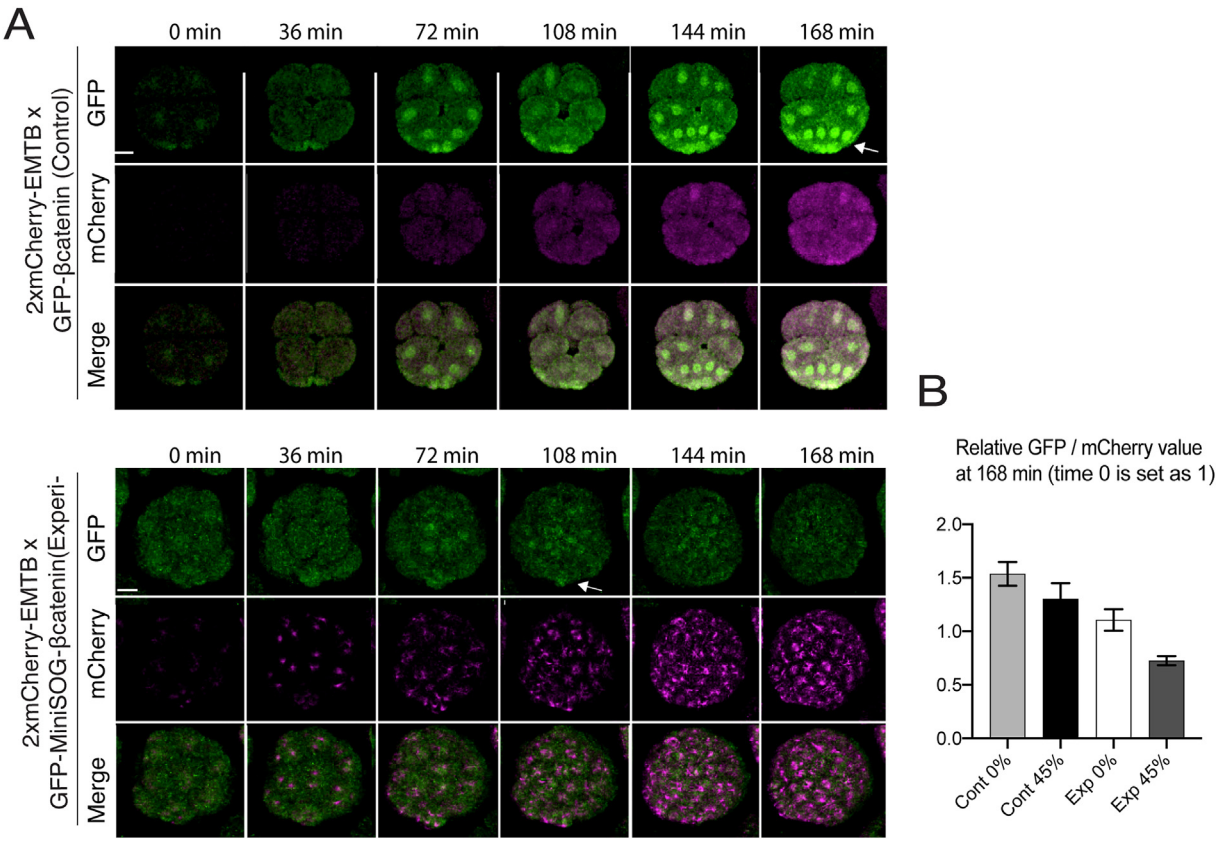

Fig. 6. CALI diminishes nuclear gradient of GFP-miniSOG-β-catenin. (A) A time-lapse series of the control (GFP- βcatenin, top panels) and experimental (GFP-miniSOG-β-catenin, bottom) group embryos. Minutes after blue laser irradiation (45%) are indicated at the top of each panel. 2xmCherry-EMTB (magenta) was used as a base control. Control group showed nuclear gradient of β-catenin overtime yet experimental group failed to show the gradient (arrows). (B) Average relative intensity value of each embryo group at the time point of 168 min is summarized. n = 4. Scale bars = 20 μm.

yet they may not be ideal for long-term lineage tracing. Modifications of existing or a new line of photoconvertible proteins with a longer protein stability will be necessary for a successful use of photoconvertible proteins as lineage tracers in the future.

To dissect a subcellular function of a protein of interest, CALI was tested in this study. We demonstrate that, using two different laser microscopes (Olympus FV3000 and Nikon W1 Spinning Disk scopes), MiniSOG may be a promising CALI tool to dissect protein function and further to control a cellular activity such as asymmetric cell division. Conventional knockdown approaches using siRNA or morpholino antisense oligo inhibit activities of the target protein in the entire embryo throughout development. Therefore, these conventional approaches do not allow one to test protein's function at each site and/or at each timepoint, while CALI could inactivate the function of a protein at a subcellular level with a spatial and temporal precision, providing another level of molecular and cellular analyses.

The major hurdle of the CALI technology has been, however, to identify or engineer the CALI protein that can produce the maximum amount of ROS to destroy the protein of interest with a minimum light irradiation (Sano et al., 2014). MiniSOG was selected due to its small size and its effective CALI activities demonstrated in the area of neuroscience (Qi et al., 2012; Lin et al., 2013). However, it still required a significant amount of blue laser power, ~45% power in our hands, to see a significant signal reduction of the miniSOG-fusion protein both on the FV3000 and W1 scopes, or ~80% power to block micromere formation on the Nikon W1 scope. This is notable compared to the previously demonstrated LOV-ePDZ optogenetic system that typically required only ~10% laser irradiation on the same FV3000 scope (Uchida and Yajima, 2018). In the current study, however, embryos successfully developed under this strong blue laser irradiation, suggesting that the CALI system may still be useful in some applications. For example, this technology might be useful to transiently deplete a protein of interest at a subcellular level, so the laser irradiation and its cytotoxicity will be more restricted. In this study, depletion of GFP-miniSOG-AGS considerably delayed or inhibited the rescue of asymmetric cell division, while the sibling non-irradiated blastomere within the same embryo showed no apparent delay or failure in cell division. Since AGS functions both in symmetric and asymmetric cell divisions in the entire embryo, a general knockdown of AGS disturbs all cell divisions (Poon et al., 2019). CALI here provides a spatial and temporal control of AGS inactivation specifically at the vegetal cortex during an asymmetric cell division, testing and revealing for the first time a direct contribution of AGS to micromere formation at 16-cell stage. Based on this observation, future experiments could address how AGS directly controls micromere formation. Therefore, CALI could be a useful tool to dissect protein function in time and space.

To increase efficacy and versatility of the CALI technology, however, further technological development might be needed. For example, more advanced control of laser irradiation that takes into account the three-dimensionality of the embryo will help improve efficacy of CALI in the future. The current laser irradiation system on the microscope typically targets specific x- and y-areas but penetrates the entire z-sections with the best focus on the specific z-plane. Therefore, the laser condition needs to be carefully adjusted to induce targeted activation but not unwanted activation at the specific z-plane, which is often technically challenging because each embryo changes its orientation and/or undergoes cell divisions in real-time while imaging. In this study, therefore, only a specific z-plane within an entire patch of the AGS signal at the vegetal cortex was irradiated per laser shot, which required multiple laser shots to see notable outcomes. Further, the current CALI approach requires co-introduction of morpholino antisense oligo to reduce the contribution

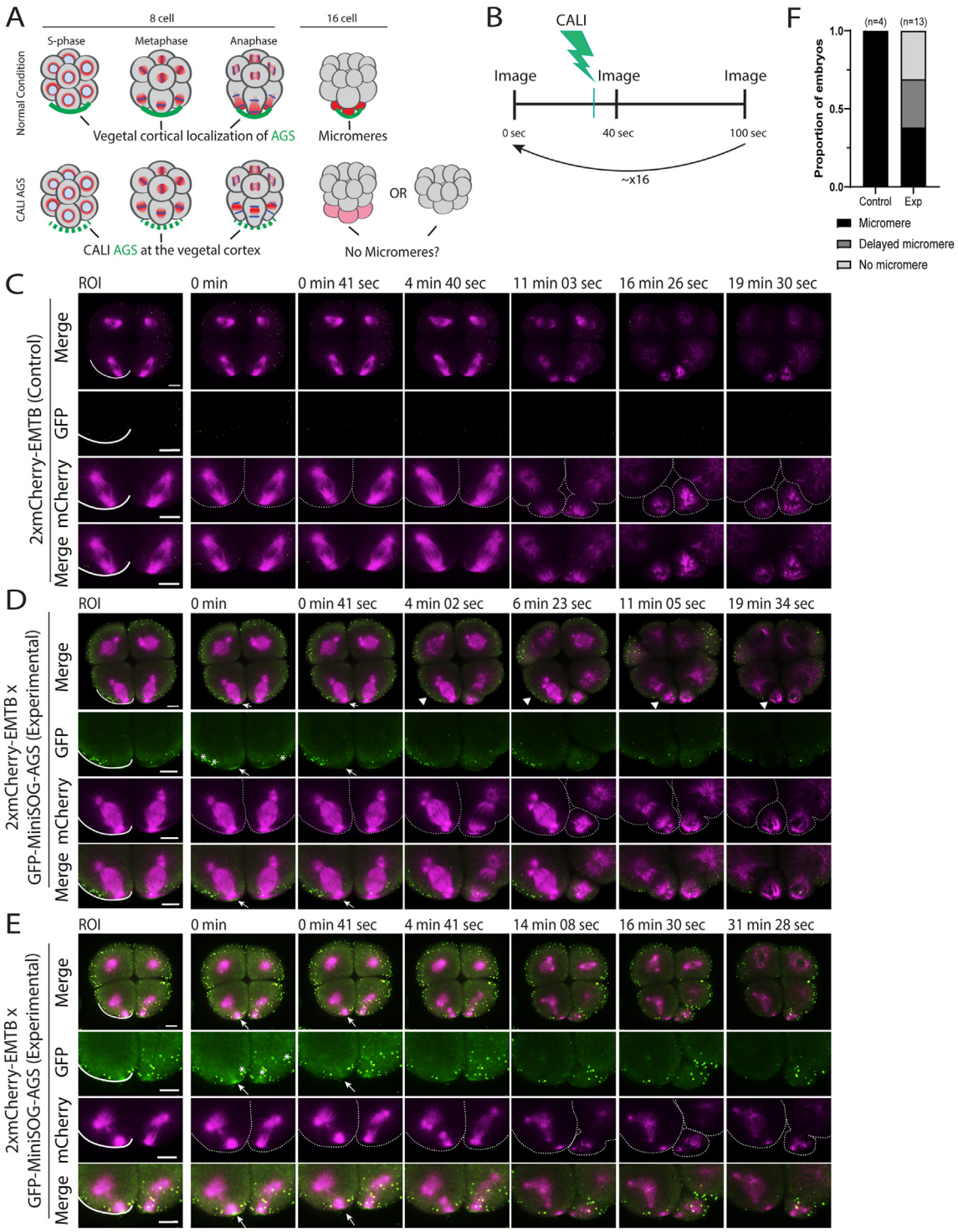

Fig. 7. AGS-CALI disrupts asymmetric cell division. (A) Top panel, A schematic diagram indicating AGS (green) localization that regulates asymmetric cell division (micromere formation) at the vegetal cortex in normal development. Bottom panel, A hypothetical scenario of asymmetric cell division failure when AGS is lost from the cortex. (B) A schematic diagram of experimental procedure. (C–E) Representative time-lapse images of each phenotype observed. The leftmost column of images indicates the ROI in white used for blue laser irradiation to induce CALI. Images were taken every 40–60 s at 1 μm z-stack interval and 2D-projection images of the indicated timepoints are shown. For each embryo, the top panel represents the full embryo with merged channels. The following three panels represent a magnified view of the vegetal pole for each channel and merged channels. (C) Control embryo showed proper micromere formation from the targeted blastomere. (D) Experimental embryo showed delayed micromere formation from the irradiated blastomere compared to the sibling blastomere. Delayed division is indicated by arrowhead. (E) Experimental embryo failed to form a micromere from the irradiated blastomere while the non-targeted sibling blastomere divided properly. Arrow points to AGS signal before and after CALI. Asterisks indicate non-specific signal from microscope. Green, AGS; Magenta, tubulin. Scale bars = 10 μm. (F) Proportion of embryos making micromeres, delayed micromeres or no micromeres following blue laser irradiation in the 2xmChEMTB injected control group (n = 4) or in the experimental group injected with GFP-miniSOG-AGS (n = 13).

of endogenous protein in the cell. Since a controlled balance of miniSOG-tagged mRNA and morpholino antisense oligo is critical to maximize the CALI efficacy, the target proteins may be limited to those that are well characterized in previous studies such as AGS used in this study. Therefore, the CALI approach may be more suitable for advanced studies to dissect further the spatial and temporal function of a well-characterized protein of interest at current settings. In the future, however, CALI technology could be combined with the CRISPR-mediated genome editing technology (Lin and Su, 2016; Lin et al., 2019). Recent effort in the field to construct genetic lines of the genome-edited sea urchin is promising (Wessel et al., 2020; Yaguchi et al., 2020), which could remove the need of morpholino or exogenous mRNA introduction in the future.

Overall, these light-induced approaches are useful to dissect the function and/or activity of the protein at a subcellular level. Each of these optogenetic tools provides different advantages and obstacles, which should be carefully considered based on the desired application and outcomes. Many genes and proteins are repeatedly used in various cell types and biological contexts during development of many organisms. Therefore, the ability to manipulate a subset of proteins at specific time and space is critical to understand their direct roles and behaviors in each biological process. Light-induced approaches have a great potential to address these cellular and developmental questions that were previously not addressable through conventional gene/protein knockdown approaches. We hope the experimental details covered in this study help facilitate a use of these technologies in our research community and beyond.

Acknowledgements

We thank members of PRIMO at Brown University for general discussion of the manuscript. J.P., F.L. were responsible for experimental design and undertaking, data analysis, and manuscript construction; G.W. was responsible for experimental design and manuscript editing; M.Y. was responsible for conceptualization, experimental design and undertaking, manuscript construction and editing. This work was supported by the American Heart Association Scientist Development Grant (#14SDG18350021), the National Institute of General Medical Sciences (1R01GM126043-01 to M.Y. and RO1GM125071 to G.M.W.) and the National Science Foundation (IOS-1940975 to M.Y. and IOS-1923445 to G.M.W.).

Appendix A. Supplementary data

Supplementary data to this article can be found online at https://doi.org/10.1016/j.ydbio.2021.06.006.

References

Adam, V., Nienhaus, K., Bourgeois, D., Nienhaus, G.U., 2009. Structural basis of enhanced photoconversion yield in green fluorescent protein-like protein Dendra2. Biochemistry 48, 4905–4915.

Ando, R., Hama, H., Yamamoto-Hino, M., Mizuno, H., Miyawaki, A., 2002. An optical marker based on the UV-induced green-to-red photoconversion of a fluorescent protein. Proc. Natl. Acad. Sci. U.S.A. 99, 12651–12656.

Diamond, P., Mallavarapu, A., Schnipper, J., Booth, J., Park, L., O'Connor, T.P., Jay, D.G., 1993. Fasciclin I and II have distinct roles in the development of grasshopper pioneer neurons. Neuron 11, 409–421.

Jacobson, K., Rajfur, Z., Vitriol, E., Hahn, K., 2008. Chromophore-assisted laser inactivation in cell biology. Trends Cell Biol. 18, 443–450.

Jay, D.G., 1988. Selective destruction of protein function by chromophore assisted laser inactivation. Proc. Natl. Acad. Sci. U.S.A. 85, 5454–5458.

Liao, J.C., Roider, J., Jay, D.G., 1994. Chromophore-assisted laser inactivation of proteins is mediated by the photogeneration of free radicals. Proc. Natl. Acad. Sci. U.S.A. 91, 2659–2663.

Lin, J.Y., Sann, S.B., Zhou, K., Nabavi, S., Proulx, C.D., Malinow, R., Jin, Y., Tsien, R.Y., 2013. Optogenetic inhibition of synaptic release with chromophore-assisted light inactivation (CALI). Neuron 79, 241–253.

Lin, C.Y., Su, Y.H., 2016. Genome editing in sea urchin embryos by using a CRISPR/Cas9 system. Dev. Biol. 409, 420–428.

Lin, C.Y., Oulhen, N., Wessel, G., Su, Y.H., 2019. CRISPR/Cas9-mediated genome editing in sea urchins. Methods Cell Biol. 151, 305–321.

Logan, C.Y., Miller, J.R., Ferkowicz, M.J., McClay, D.R., 1999. Nuclear b-catenin is required to specify vegetal cell fates in the sea urchin embryo. Development 126, 345–357.

McKinney, S.A., Murphy, C.S., Hazelwood, K.L., Davidson, M.W., Looger, L.L., 2009. A bright and photostable photoconvertible fluorescent protein. Nat. Methods 6, 131–133.

Miller, A.L., Bement, W.M., 2009. Regulation of cytokinesis by Rho GTPase flux. Nat. Cell Biol. 11, 71–77.

Mizuno, H., Mal, T.K., Tong, K.I., Ando, R., Furuta, T., Ikura, M., Miyawaki, A., 2003. Photo-induced peptide cleavage in the green-to-red conversion of a fluorescent protein. Mol. Cell 12, 1051–1058.

Nowotschin, S., Hadjantonakis, A.K., 2009. Use of KikGR a photoconvertible green-to-red fluorescent protein for cell labeling and lineage analysis in ES cells and mouse embryos. BMC Dev. Biol. 9, 49.

Poon, J., Fries, A., Wessel, G.M., Yajima, M., 2019. Evolutionary modification of AGS protein contributes to formation of micromeres in sea urchins. Nat. Commun. 10, 3779.

Qi, Y.B., Garren, E.J., Shu, X., Tsien, R.Y., Jin, Y., 2012. Photo-inducible cell ablation in Caenorhabditis elegans using the genetically encoded singlet oxygen generating protein miniSOG. Proc. Natl. Acad. Sci. U.S.A. 109, 7499–7504.

Rajfur, Z., Roy, P., Otey, C., et al., 2002. Dissecting the link between stress fibres and focal adhesions by CALI with EGFP fusion proteins. Nat. Cell Biol. 4, 286–293.

Sano, Y., Watanabe, W., Matsunaga, S., 2014. Chromophore-assisted laser inactivation - towards a spatiotemporal functional analysis of proteins, and the ablation of chromatin, organelle and cell function. J. Cell Sci. 127 (Pt 8), 1621–1629(. . Review.).

Schmidt, A., Wiesner, B., Schulein, R., Teichmann, A., 2014. Use of Kaede and Kikume green-red fusions for live cell imaging of G protein-coupled receptors. Methods Mol. Biol. 1174, 139–156.

Shevidi, S., Uchida, A., Schudrowitz, N., Wessel, G.M., Yajima, M., 2017. Single nucleotide editing without DNA cleavage using CRISPR/Cas9-deaminase in the sea urchin embryo. Dev. Dynam. 246, 1036–1046.

Subach, F.V., Patterson, G.H., Manley, S., Gillette, J.M., Lippincott-Schwartz, J., Verkhusha, V.V., 2009. Photoactivatable mCherry for high-resolution two-color fluorescence microscopy. Nat. Methods 6, 153–159.

Tour, O., Meijer, R.M., Zacharias, D.A., Adams, S.R., Tsien, R.Y., 2003. Genetically targeted chromophore-assisted light inactivation. Nat. Biotechnol. 21, 1505–1508.

Trewin, A.J., Berry, B.J., Wei, A.Y., Bahr, L.L., Foster, T.H., Wojtovich, A.P., 2018. Light-induced oxidant production by fluorescent proteins. Free Radic. Biol. Med. 128, 157–164.

Tsutsui, H., Karasawa, S., Shimizu, H., Nukina, N., Miyawaki, A., 2005. Semi-rational engineering of a coral fluorescent protein into an efficient highlighter. EMBO Rep. 6, 233–238.

Uchida, Alicia, Yajima, Mamiko, 2018. An optogenetic approach to control protein localization during embryogenesis of the sea urchin. Dev. Biol. https://doi.org/10.1016/j.ydbio.2018.06.015.

von Dassow, G., Verbrugghe, K.J., Miller, A.L., Sider, J.R., Bement, W.M., 2009. Action at a distance during cytokinesis. J. Cell Biol. 187, 831–845.

Wei, Z., Angerer, R.C., Angerer, L.M., 2011. Direct development of neurons within foregut endoderm of sea urchin embryos. Proc. Natl. Acad. Sci. U. S. A. 108, 9143–9147.

Wessel, G.M., Kiyomoto, M., Shen, T.L., Yajima, M., 2020. Genetic manipulation of the pigment pathway in a sea urchin reveals distinct lineage commitment prior to metamorphosis in the bilateral to radial body plan transition. Sci. Rep. 10, 1973.

Wolf, H., Barisas, B.G., Dietz, K.J., Seidel, T., 2013. Kaede for detection of protein oligomerization. Mol. Plant 6, 1453–1462.

Yaguchi, S., Yaguchi, J., Suzuki, H., Kinjo, S., Kiyomoto, M., Ikeo, K., Yamamoto, T., 2020. Establishment of homozygous knock-out sea urchins. Curr. Biol. 30, R427–R429.

Yajima, M., Wessel, G.M., 2011. The DEAD-box RNA helicase Vasa functions in embryonic mitotic progression in the sea urchin. Development 138, 2217–2222.

Yajima, M., Wessel, G.M., 2015. The germ line factor Vasa functions broadly in somatic cells: mRNA clustering, translational regulation, and wound healing. Development 142, 1960–1970.